ISSN 0023-1584, Kinetics and Catalysis, 2006, Vol. 47, No. 5, pp. 776–781. © MAIK "Nauka/Interperiodica" (Russia), 2006.
Original Russian Text © Yu.I. Aristov, I.V. Koptyug, L.G. Gordeeva, L.Yu. Il'ina, I.S. Glaznev, 2006, published in Kinetika i Kataliz, 2006, Vol. 47, No. 5, pp. 799–804.

Dynamics of Water Vapor Sorption in a $CaCl_2$/Silica Gel/Binder Bed: The Effect of the Bed Pore Structure

Yu. I. Aristov[a], I. V. Koptyug[b], L. G. Gordeeva[a], L. Yu. Il'ina[b], and I. S. Glaznev[a]

[a] *Boreskov Institute of Catalysis, Siberian Branch, Russian Academy of Sciences, Novosibirsk, 630090 Russia*
[b] *International Tomography Center, Siberian Branch, Russian Academy of Sciences, Novosibirsk, 630090 Russia*
e-mail: aristov@catalysis.ru

Received February 10, 2005

Abstract—The dynamics of water vapor sorption in a compact, binder-containing bed of a $CaCl_2$-in-silica-gel-pores sorbent has been investigated by NMR microscopy. The procedure suggested for the preparation of this bed allows the porous structure of the bed to be modified in a wide range. The bed pore structure and water transfer in the bed have been studied in relation to the particle size of the initial silica gel, the size of mesopores in the sorbent particles, and the binder content. By varying these parameters, it is possible to optimize the ratio of the diffusion resistance of the interparticle macropores to that of the internal mesopores of the particles. If sorption is controlled by water diffusion in the macropores, a sorption front forms in the sample to move inside the bed. The distance traveled by the front is proportional to the sorption time to the power 1/2. The effective diffusion coefficient of water in the macropores is estimated from the front motion dynamics to be between 0.8×10^{-9} and 3.0×10^{-9} m^2/s, depending on the porous structure of the bed.

DOI: 10.1134/S0023158406050181

Adsorption heat pumps (AHPs) are considered to be a real alternative to compression pumps, because they do not use gases contributing to the greenhouse effect or damaging the ozone layer [1, 2]. Many laboratories are now developing efficient AHPs employing water, an environmentally friendly liquid, as the adsorbate [1, 2]. Among the central problems encountered in this approach is that of ensuring efficient heat and mass transfer during water sorption in the sorbent bed. Efficient heat supply is usually achieved using not a granular bed of free-lying sorbent particles but a more compact sorbent bed prepared by "gluing" the initial sorbent particles with a binder (Fig. 1a). The binder and the increased bed density favor heat transfer but can deteriorate the water vapor mass transfer. If this is the case, the mass transfer will control the water sorption kinetics. In an isothermal regime, the sorption kinetics depends mainly on the ratio (α) of the diffusion constant for the macropores formed between initial adsorbent particles of size A (transport pores) to the diffusion constant for the internal mesopores or micropores of these particles. The former constant, $k_{D(macro)} = D_{macro}/L^2$, where D_{macro} is the diffusion coefficient of water vapor in the macropores and L is the bed thickness, determines the characteristic time of water sorption in the bed, $\tau = 1/k_{D(macro)}$. The diffusion constant for the interior of an initial particle is $k_{D(meso)} = D_{meso}/\bar{R}^2$, where D_{meso} is the diffusion coefficient for the mesopores of the initial particle and $\bar{R}$ is the average particle radius ($\bar{R} = A/2$). If $\alpha = (D_{macro}/L^2)/(D_{meso}/\bar{R}^2) \ll 1$, the equilibrium inside the initial sorbent particles is rapidly established and the sorption rate is determined by diffusion in the macropores of the bed. Analytical equations have been set up for this case, which describe the time dependence of the amount of sorbed water for both isothermal and nonisothermal regimes [3].

At $\alpha \ll 1$, a profile of sorbed water forms to travel into the bed bulk (Fig. 1b). Knowing the shape and position of the front as a function of time, one can find, by the Boltzmann–Matano method, the effective water diffusion coefficient [4].

In the opposite case ($\alpha \gg 1$), a constant water vapor concentration equal to the water concentration over the bed is rapidly established in the gas phase and moisture is almost uniformly distributed throughout the bed (Fig. 1d). The water sorption kinetics in the bed will then be determined by the way water is sorbed by individual particles (under the assumption that the binder does not block access to the outer particle surface). It is possible to measure kinetics of water sorption on an isolated particle by a separate experiment [5] and to use the results in the kinetic analysis of water sorption in the bed.

If the diffusion resistances in the macropores and mesopores are comparable ($\alpha \approx 1$), the sorption profiles have a more complicated shape (Fig. 1c) and detailed mathematical modeling is required for their description.

In the study reported here, we varied the diffusion constant ratio α by widely varying, at the synthesis stage, the basic bed parameters that can affect the

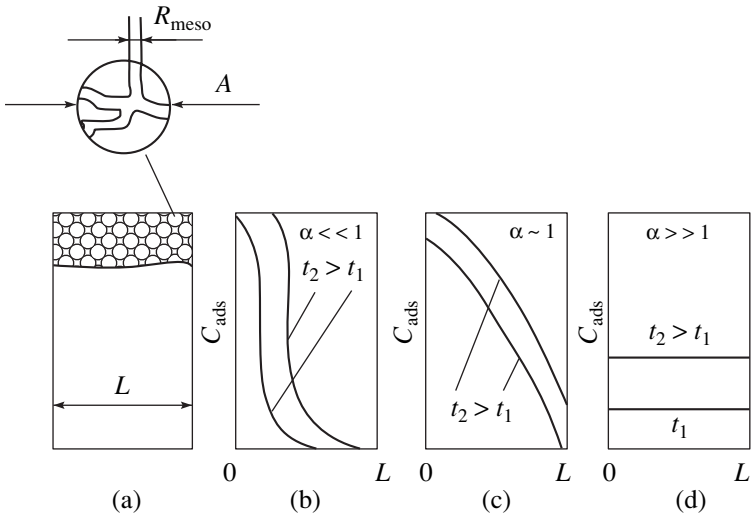

Fig. 1. (a) Bed consisting of initial particles of size *A*. (b–d) Sorbed water profiles depending on the ratio of macropore and mesopore diffusion resistances.

porous structure of the bed, namely, the initial particle size of the sorbent, the size of mesopores in the particles, and the amount of binder.

Water vapor mass transfer in the bed was studied by NMR microscopy, which enabled us to visualize the space and time profiles of sorbed water without breaking the sample [6, 7]. The object of our study was a calcium chloride/silica gel composite sorbent (SWS-1K) [8–10]. Although this new material has only recently been suggested for AHP applications [11, 12], it has already demonstrated its high efficiency in adsorption systems for cooling water to 5–10°C in which the heat source has a low temperature potential (80–90°C) [13]. In order to optimize the dynamic characteristics of such a device, it is necessary to study water vapor transfer in a compact SWS-1K bed with a binder. This process is the subject of the present study.

EXPERIMENTAL

Sample Preparation

Initially, we determined the basic parameters that might have an effect on the bed pore structure and, accordingly, on water vapor transfer in the bed: the mean size of initial silica gel particles (*A*), the mean size of the mesopores in these particles (R_{meso}), and the binder content ([B]). In the Knudsen regime, the diffusion resistance in the initial particle depends on the mesopore size; for this reason, silica gels with two different mesopores sizes, R_{meso} = 3.0 and 7.5 nm, were used in the bed preparation. The particle size *A* and the binder content [B] have an effect on the average size R_{macro} (or volume) of pores between initial powder particles (i.e., on the parameters of transport macropores). The diffusion resistance of these pores decreases with increasing size of initial particles and with decreasing binder content.

Next, we obtained beds while systematically varying the above three parameters. The host matrices were the silica gels KSK, Davisil Grade 635, Davisil Grade 645, and Grace SP2-8926.02, whose properties are listed in Table 1. A certain fraction of oxide powder and a binder were dispersed in water containing 1% nitric acid. The binder was pseudoboehmite. Its content [B] was varied between 10 and 30 wt %. The dispersion was homogenized with a Cool Parmer 8890 ultrasonic disperser for 1 h while stirring with a mechanical stirrer. The excess water was evaporated to a water content of 45–55%, and the resulting paste was shaped into pellets 16 mm in diameter and 6 mm in thickness. The pellets were air-dried at 450°C, impregnated with an aqueous calcium chloride solution, and dried at 150°C. The salt contents of the resulting materials are listed in Table 2.

Pore-size distribution for all materials was determined by mercury porosimetry using a Micromeritics Pore Size 9300 instrument. Micrographs were obtained with an REM-100U scanning electron microscope with a digital image output system, using an accelerating voltage of 30 kV. Prior to microscopic examination, gold was thermally sputtered onto the specimen surface in vacuo to obtain a thin conducting film. The mechanical strength of the films was evaluated from crushing load data.

Mass Transfer Measurements

In order to estimate the spatial distribution of sorbed water in a pellet, the pellet was placed into the measurement cell of an Avance Brucker NMR tomograph [14] (Fig. 2). The cell was pumped and was then connected

Table 1. Properties of silica gels used in the preparation of compact beds

Silica gel	S_{sp}, m^2/g	V_{por}, cm^3/g	A, μm	R_{meso}, nm
Davisil Grade 635	490	0.95	150–250	3.0
Davisil Grade 645	300	1.15	150–250	7.5
Grace SP2-8926.02	325	1.50	40–60	7.5
KSK	340	1.00	variable	7.5

Note: The specific surface area S_{sp}, pore volume V_{por}, and mean mesopore radius R_{meso} were measured by nitrogen porosimetry. A is the average particle size.

to a thermostated evaporator containing a saturated calcium chloride solution. A constant water vapor pressure of 7 mbar was maintained over the solution. Only the upper flat surface of the pellet was accessible to water vapor. The sample temperature was 18–19°C. The determination of time-dependent sorbed water profiles is described elsewhere [14]. The space resolution was 50–70 μm. The time required for recording one profile (2–5 min) was sufficiently short for studying the diffusion processes, whose duration is tens or even hundreds of minutes, as will be demonstrated below.

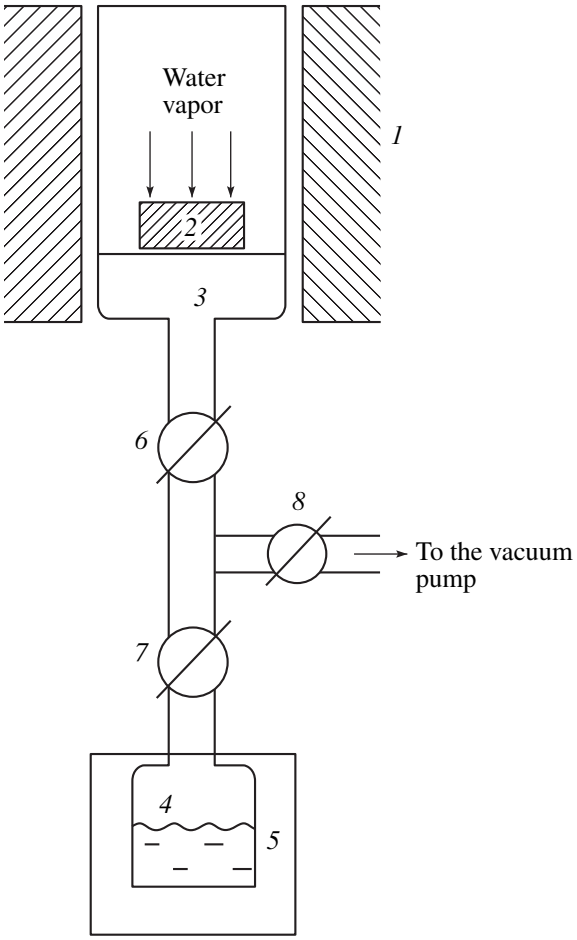

Fig. 2. Experimental setup for studying water vapor adsorption in a sorbent bed: (*1*) measurement cell of an NMR tomograph, (*2*) sample, (*3*) water-vapor-permeable sample holder, (*4*) evaporator containing a $CaCl_2$ solution, (*5*) thermostat, and (*6–8*) vacuum valves.

RESULTS AND DISCUSSION

Porous Structure of the Materials

The mesoporous structure of the starting silica gels is characterized by a comparatively narrow pore-size distribution with a mean pore diameter of 6 or 15 nm (Table 1). Note that the heat treatment of pseudoboehmite yields pores similar in size to silica gel pores. Therefore, the binder causes no significant changes in the mesoporous structure of the starting silica gel particles.

The structure of transport pores depends most strongly on A and [B]. The materials with [B] < 20 wt % had a low mechanical strength (Table 2). For this reason, [B] in most cases was varied between 20 and 30 wt %. In this binder content range, the volume of transport pores in the bed (R_{macro} > 0.1 μm) is nearly constant, but the size distribution of these pores changes (Fig. 3). In the bed that was prepared from 150- to 250-μm particles and has a binder content of [B] = 20 wt %, the size of

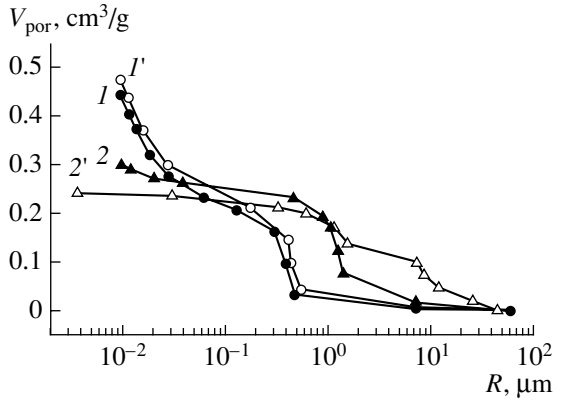

Fig. 3. Pore-size distribution for a binder-containing compact bed. The particle size of the original silica gel is (*1*, *1'*) 40–60 and (*2*, *2'*) 150–250 μm. The binder content is (*1'*, *2'*) 20 and (*1*, *2*) 30 wt %.

most of the transport pores is 2 to 30 μm (Fig. 3). At [B] = 30 wt %, pores greater than 6–10 μm are almost absent and most of the transport pores have a size of 0.7 to 6 μm. This is apparently due to the binder filling part of the interparticle space. At A = 40–60 μm, the dominant transport pores have a still smaller size of 0.4–1.0 μm (Fig. 3). The volume of the transport pores depends only weakly on the size of the initial particles and the binder content and is 0.24–0.28 cm^3/g, ~2 times smaller than the pore volume of a bed of free-lying silica gel particles.

Let us compare the size of transport macropores observed in the binder-containing bed to the macropore size theoretically calculated for a bed of free-lying spherical particles of diameter D (i.e., for a bed without a binder). Theory predicts that the mean size of intersphere pores will be $d = (2/3)[\varepsilon/(1-\varepsilon)]D$, where ε is the bed porosity [15]. In a random dense packing of spheres, ε = 0.36–0.40 and, accordingly, d = (0.375–0.440)D. For the mean particle sizes of D = 50 and 200 μm, we obtain d = 19–22 and 75–90 μm, respectively. For the size fraction of 150–250 μm, the macropore size observed in the bed is smaller than the theoretical pore size by a factor of 2–6 for [B] = 20 wt % and by a factor of 15–100 for [B] = 30 wt %. A qualitatively similar situation is observed for the 40- to 60-μm size fraction. Thus, it is likely that the binder not only fills a considerable part of the space between initial silica gel particles, thereby reducing the macropore volume, but also markedly diminishes the size of the transport pores capable of transferring water vapor.

Another possible cause of the observed macropore size being so far below the theoretical value is that the initial silica gel particles break into smaller ones during mechanical processing, resulting in a decrease in the free interparticle volume.

An SEM examination of the texture of the sorbents confirmed the data obtained by mercury porosimetry. It is clear from SEM images that raising the binder content from 10 to 30 wt % causes the binder to fill the pore space (Fig. 4). The micrographs of the specimens prepared from the 40- to 60-μm size fraction of silica gel display particles with a substantially smaller diameter, which are likely to have resulted from the breaking of initial silica gel particles.

Table 2. Mechanical strength of synthesized beds with various binder and salt contents

Silica gel	[B], wt %	[$CaCl_2$], wt %	Mechanical strength, kg/cm^2
Davisil Grade 635	20	31.1	–
	30	22.9	68.2
Grace SP2-8926.02	20	38.1	76.4
	30	30.5	120.1
Davisil Grade 645	20	33.0	64.6
	30	30.0	68.9

Water Vapor Mass Transfer

Water mass transfer in a compact SWS-1K bed with a binder was studied by NMR microscopy, recording the spatial distribution of sorbed water as a function of time. It was found that a sorption front forms in the bed to move into the sample bulk with some deceleration.

Figure 5 shows typical sorbed water profiles for a bed prepared of two silica gels with the same initial particle size (150–250 μm) and different sizes of internal mesopores (R_{meso} = 3.0 and 7.5 nm). These materials show nearly the same water sorption dynamics, which, therefore, depends only slightly on the mesopore size. Therefore, sorption is controlled by water transfer in the bed macropores rather than by water transfer in the internal mesopores of the initial particles. In the first approximation, the front displacement x as a function of time t is proportional to $t^{1/2}$ for 1.5 h ≤ t ≤ 6 h (Fig. 6). This is typical of diffusion processes. From the slope of the x^2 versus t straight line, the effective water diffusion coefficient for the bed was estimated to be $D_{eff} = 1.2 \times 10^{-9}$ m^2/s. At [B] = 30 wt %, water reaches the rear end of a 6-mm-thick bed in 6 h (Fig. 5).

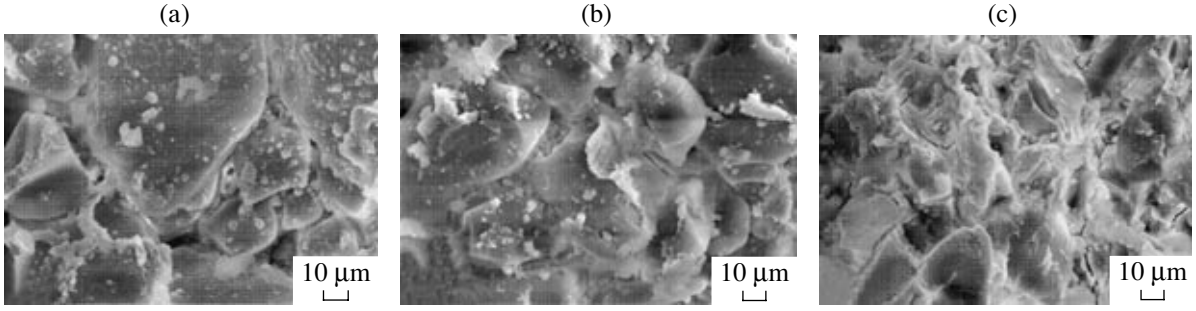

Fig. 4. Electron micrographs of binder containing compact beds prepared from the 40- to 60-μm size fraction of silica gel. The binder content is (a) 10.0, (b) 20.0, and (c) 30.0 wt %.

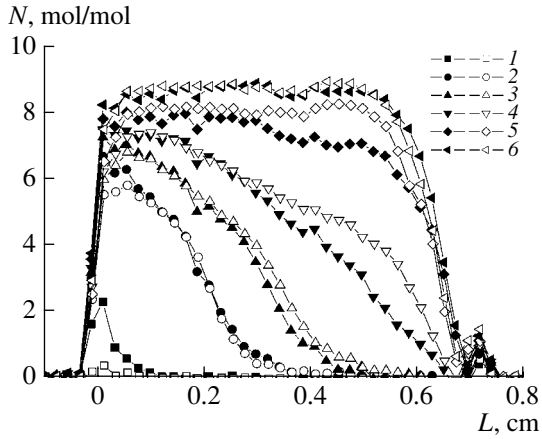

Fig. 5. Time-dependent profiles of sorbed water in compact beds of silica gel particles (150- to 250-μm size fraction) with R_{meso} = 3.0 nm (dark symbols) and 7.5 nm (light symbols). The binder content is 30 wt %. Time elapsed from the beginning of the process: (*1*) 10 min 50 s, (*2*) 1 h 37 min, (*3*) 3 h 4 min, (*4*) 5 h 57 min, (*5*) 13 h 11 min, and (*6*) 17 h 30 min.

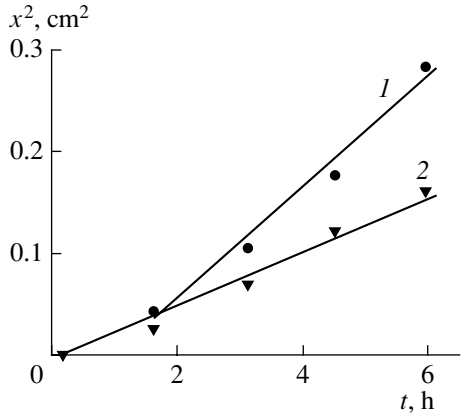

Fig. 6. Squared displacement of the water sorption front as a function of sorption time for (*1*) Davisil Grade 645 and (*2*) Grace SP2-8926.02 silica gel beds containing 20% binder.

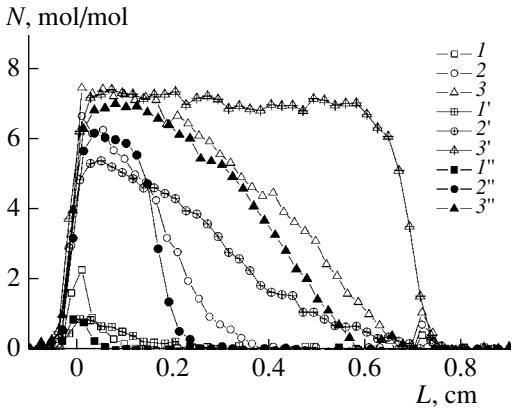

Fig. 7. Sorbed water profiles for binder-containing SWS-1K beds at sorption times of (*1*, *1*', *1*") 10 min 50 s, (*2*, *2*', *2*") 1 h 37 min, and (*3*, *3*', *3*") 5 h 57 min: (*1–3*) particle size 150–250 μm, 20 wt % binder; (*1*'–*3*') particle size 150–250 μm, 30 wt % binder; (*1*"–*3*") particle size 40–60 μm, 20 wt % binder.

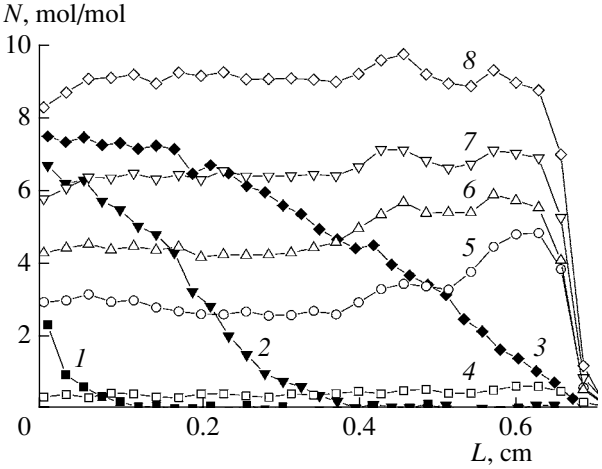

Fig. 8. (*1–3*) Sorbed water profiles for a binder-containing SWS-1K bed (particle size 150–250 μm, 30 wt % binder) at sorption times of (*1*) 11 min, (*2*) 1 h 37 min, and (*3*) 5 h 57 min. (*4–8*) The same for a bed of free-lying SWS-1K granules without a binder at sorption times of (*4*) 11 min, (*5*) 37 min, (*6*) 54 min, (*7*) 1 h 37 min, and (*8*) 5 h 52 min.

Reducing the binder content to 20 wt % increases the size of transport pores (Fig. 3), enhancing the water vapor mass transfer in the bed (Fig. 6). It takes ~1.5 h for the first water portions to diffuse through the bed thickness, and equilibrium is established in the bed in 6 h (Fig. 7). In this case, the effective diffusion coefficient exceeds (2.5–3.0) × 10^{-9} m^2/s. The sorbed water profile is widened, and its shape indicates that the above-mentioned diffusion resistances are comparable. Accordingly, the sorption rate depends on water vapor mass transfer both in the macropores between initial particles and in the internal mesopores of these particles (Fig. 1c). If no binder is present, water vapor is sorbed uniformly throughout the bed of free-lying of SWS-1K granules (Fig. 8). The kinetics of this process is determined by water vapor mass transfer in the mesopores of the individual particles constituting the bed (Fig. 1d).

Reducing the particle size of the initial powder from 150–250 to 49–60 μm causes a decrease in the size of transport macropores (Fig. 3) and, accordingly, decelerates water sorption: a sorption front forms again, which moves across the bed to reach the rear end of the pellet in ~8 h (Fig. 7). The motion of the front is characterized by the effective diffusion coefficient D_{eff} = 0.8 × 10^{-9} m^2/s, which is 1.5 times smaller than

the same coefficient for a bed of 150- to 250-μm particles containing 30% binder.

Thus, we have developed a procedure for the synthesis of compact, binder-containing, calcium chloride/mesoporous silica gel sorbent beds. This procedure allows the porous structure of the bed to be modified in a wide range. By varying the binder content and the size of initial silica gel particles, it is possible to change the porous structure so greatly as to pass from the sorption regime in which the diffusion resistance of the interparticle transport pores is much higher than that of the internal mesopores of these particles to the regime in which these resistances are comparable. In the former regime, a rather narrow sorption front is formed in the sample. This front moves inside the sample, and the distance it has traveled (x) is proportional to $t^{1/2}$. An analysis of its motion dynamics has provided an estimate for the effective diffusion coefficient of water in the macropores. Depending on the pore structure of the bed, this coefficient varies between 0.8×10^{-9} and 3.0×10^{-9} m^2/s. An analysis of the results of this study is expected to provide concrete recommendations as to the optimization of the porous structure of compact, binder-containing SWS-1K beds employed in adsorption refrigerators and heat pumps.

ACKNOWLEDGMENTS

This study was supported in part by INTAS (grant no. 2003-51-6260), the Russian Foundation for Basic Research (project nos. 05-03-34762, 05-02-16953, and 04-02-81028), and the Global Energy Foundation (grant no. MG-2005/04/3). The authors are grateful to N.A. Rudin for the SEM examination of sorbents.

REFERENCES

1. Meunier, F., *Appl. Therm. Eng.*, 1998, vol. 18, p. 715.
2. Cacciola, G. and Restuccia, G., *Heat Recovery Systems & CHP*, 1994, vol. 14, no. 4, p. 409.
3. Kaerger, J. and Ruthven, D.M., *Diffusion in Zeolites and Other Microporous Solids*, New York: Wiley, 1992.
4. Crank, J., *The Mathematics of Diffusion*, Oxford: Oxford Univ. Press, 1975, p. 230.
5. Dawoud, B. and Aristov, Yu.I., *Int. J. Heat Mass Transfer*, 2003, vol. 46, p. 273.
6. Koptyug, I.V., Khitrina, L.Yu., Aristov, Yu.I., et al., *J. Phys. Chem.*, 2000, vol. 104, p. 1695.
7. Koptyug, I.V., Sagdeev, R.Z., Khitrina, L.Yu., and Parmon, V.N., *Appl. Magn. Reson.*, 2000, vol. 18, p. 13.
8. Aristov, Yu.I., Tokarev, M.M., Marko, G., Kachchiola, G., Restuchcha, D., and Parmon, V.N., *Zh. Fiz. Khim.*, 1997, vol. 71, no. 2, p. 253 [*Russ. J. Phys. Chem.* (Engl. Transl.), vol. 71, no. 2, p. 197].
9. Aristov, Yu.I., *Extended Abstract of Doctoral (Chem.) Dissertation*, Novosibirsk: Inst. of Catalysis, 2003.
10. Aristov, Yu.I., Tokarev, M.M., Cacciola, G., and Restuccia, G., *React. Kinet. Catal. Lett.*, 1996, vol. 59, no. 2, p. 325.
11. Aristov, Yu.I., Restuccia, G., Cacciola, G., and Parmon, V.N., *Appl. Therm. Eng.*, 2002, vol. 22, no. 2, p. 191.
12. Aristov, Yu.I., *Proc. V Int. Seminar on Heat Pipes, Heat Pumps, and Refrigerators*, Minsk, 2003, p. 379.
13. Restuccia, G., Freni, A., Vasta, S., and Aristov, Yu.I., *Int. J. Refrig.*, 2004, vol. 27, no. 3, p. 284.
14. Koptyug, I.V., Khitrina, L.Yu., Parmon, V.N., and Sagdeev, R.Z., *J. Magn. Reson. Imaging*, 2001, vol. 19, p. 531.
15. Kheifets, L.I. and Neimark, A.V., *Mnogofaznye protsessy v poristykh sredakh* (Multiphase Processes in Porous Media), Moscow: Khimiya, 1982.